P1.4

INVERSION EFFECTS ON MOUNTAIN LEE WAVES

Simon Vosper *, Peter Sheridan
Met Office, U.K.

1. INTRODUCTION

The effect of a sharp low-level temperature inversion on the flow over a mountain has been investigated via two-dimensional (2-D) idealised numerical model simulations. The main focus of this study is the effect of an inversion on the formation of lee waves, lee-wave rotors, low-level hydraulic jumps, upper-level wave breaking and upwind flow blocking. Severe turbulence associated with the majority of these phenomena represents a hazard to aviators in mountainous regions. This study is an extension of that recently presented by Vosper (2004).

2. DESCRIPTION OF SIMULATIONS

The simulations were conducted using the Met Office BLASIUS model. In the idealised problem considered the upwind velocity profile is independent of height (above the boundary layer) and directed normal to an isolated 2-D ridge. The upstream stratification consists of a neutral layer immediately above the ground which is capped by a sharp temperature inversion. Above the inversion the flow is stably stratified and the Brunt-Väisälä, frequency is independent of height ($N = 0.01\ \mathrm{s}^{-1}$). A range of inversion strengths (measured by the difference in potential temperature, $\Delta\theta$, across the inversion) and inversion heights, z_i, were considered. The mountain shape considered was an isolated 2-D cosine ridge with height, H, and width L, fixed at 400 m and 10 km, respectively. A no-slip lower boundary condition was employed and this gave rise to a boundary layer below the inversion. An example upstream profile is presented in Fig. 1.

Two important controlling non-dimensional parameters are the Froude number, F_i, defined in the usual way for a two-layer shallow water flow, and the ratio of mountain height to inversion height, H/z_i. The Froude number is defined as

$$F_i = \frac{\overline{U}}{\sqrt{g' z_i}}$$

*Corresponding author address: Simon Vosper, Met Office, FitzRoy Road, Exeter, Devon, EX1 3PB, U.K.; email:simon.vosper@metoffice.com

where $\overline{U}$ is the geostrophic wind speed, $g' = g\Delta\theta/\theta_0$ and θ_0 is a reference potential temperature.

3. RESULTS

Results from simulations over a range of F_i and H/z_i show that several distinct flow types occur. In general, as the inversion strength increases (F_i decreases) the following phenomena occur:

- Lee waves on the inversion
  - Stationary downstream interfacial waves on the inversion
- Lee waves with rotors
  - Surface flow reversal and recirculation beneath the lee-wave crest, as shown in Fig. 2(a) for example.
- Hydraulic jump
  - A stationary hydraulic jump occurs above the downwind foot of the mountain, as shown in Fig. 2(b) for example.

For weak inversions, where F_i is large (typically greater than unity) none of the above features are present.

As shown in Fig. 3(a) the results can be presented in terms of a flow regime diagram. This approach clearly distinguishes between the areas of parameter space where the different flow types occur. For sufficiently low inversions (high H/z_i), the highly nonlinear hydraulic jumps dominate at low F_i, while lee waves with rotors occur at slightly higher values of F_i. Note that linear theory predicts the presence of lee waves on the inversion for some of the temperature profiles used in this study. Fig. 3(a) shows that, as F_i decreases, linear theory provides a good estimate (the solid line in the figure) of when lee waves appear. However, since the wavelength of the lee waves is much shorter than the hill width in these simulations, linear theory significantly underestimates the wave amplitude.

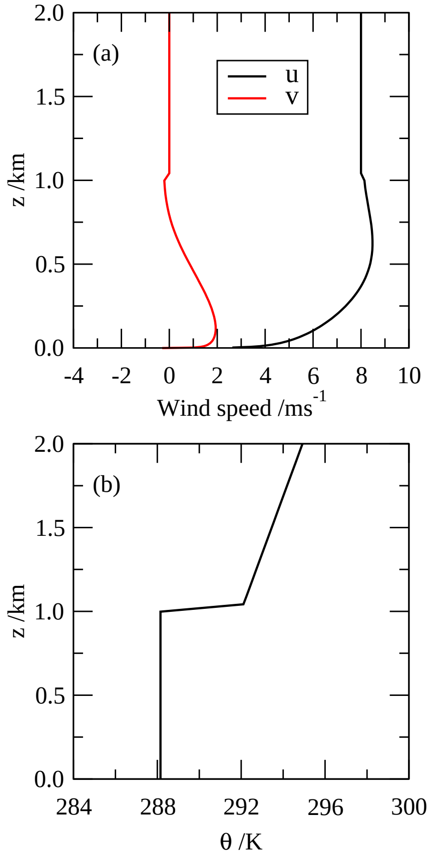

Figure 1: Profiles of (a) wind and (b) potential temperature used to initialize a 2-D simulation. In the example shown, $\Delta\theta = 3.84$ K across the inversion height, which occurs at $z_i = 1$ km. The geostrophic wind $(\overline{U}, \overline{V}) = (8, 0)\ \mathrm{ms}^{-1}$.

Simulations were also conducted using a narrower ridge, of width $L = 2.5$ km, which is closer to the resonant lee wave wavelength. In this case, it was found that, in addition to accurately predicting the wavelength of the simulated lee wave, linear theory can make a reasonable quantitative prediction of the lee-wave maximum amplitude. Linear theory also provides a useful prediction of the bound in $F_i - H/z_i$ space where surface flow reversal (i.e. lee-wave rotors) will occur (see Fig. 3(b)).

Recent observations of near-surface flow across mountains on East Falkland (south Atlantic) indicate that the presence of a strong temperature inversion influences the formation of rotors and strong downslope winds. Having constructed the regime diagrams for the above 2-D simulations, it is interesting to consider whether the approach can be useful in examining the observed 3-D flows. To this end, the flows observed on East Falkland have been categorised according to distinctive, mountain influenced near-surface flow features and values of F_i and H/z_i have been diagnosed from radiosonde profiles. Thus a flow regime diagram has been constructed for East Falkland (see accompanying paper 2.4 by Sheridan et al.). Despite the large number of complicating factors involved in categorising the observed flows, the regime diagram derived from the observations does bear some resemblance to those shown in Fig. 3.

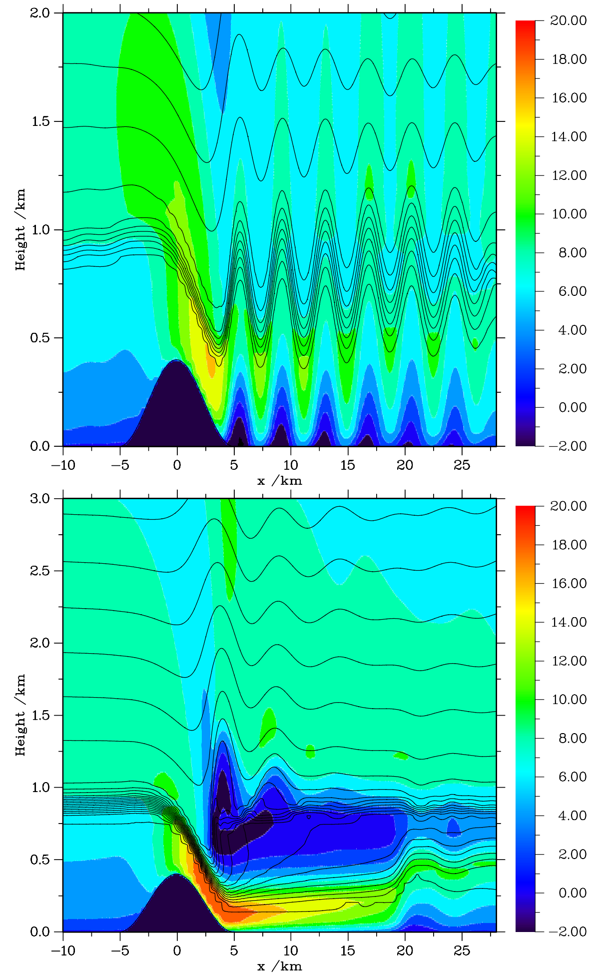

Figure 2: Flow field for flow over a hill of width $L = 10$ km, with $H/z_i = 0.5$ ($z_i = 800$ m) and (a) $F_i = 0.6$ ($\Delta\theta = 6.53$ K) and (b) $F_i = 0.4$ ($\Delta\theta = 14.69$ K). Colour shaded contours represent the streamwise velocity component and line contours show the potential temperature (interval 1 K).

4. REFERENCES

Vosper, S.B., 2004: Inversion effects on mountain lee waves. *Q. J. R. Meteorol. Soc.*, in press.

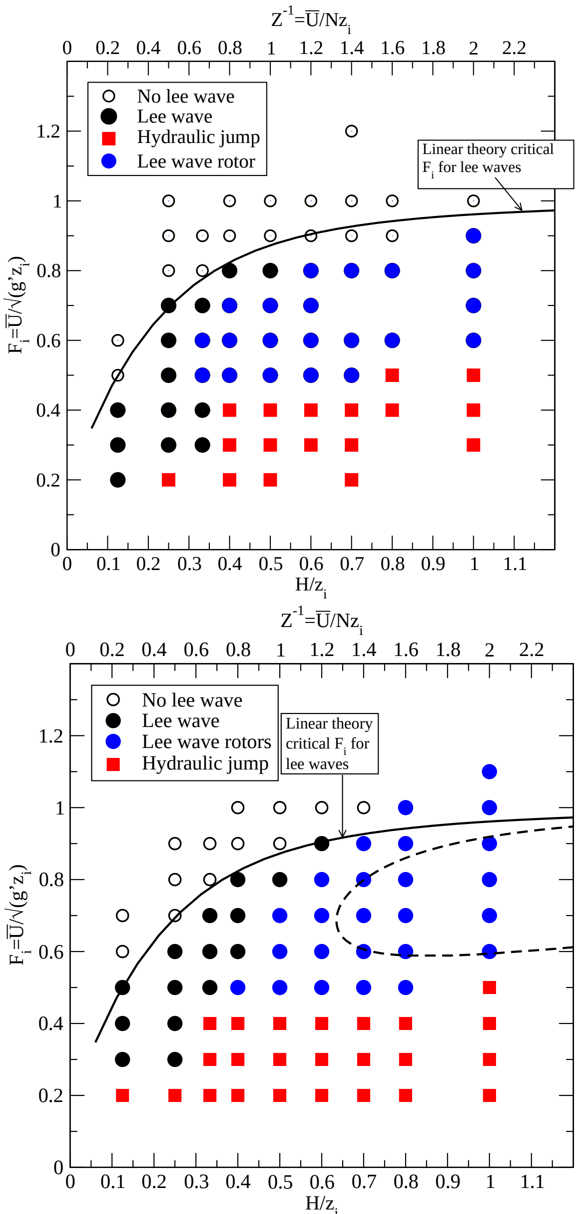

Figure 3: Regime diagrams showing the F_i and H/z_i dependence of the flow for hill widths, L, of (a) 10 km and (b) 2.5 km. The solid curve represents the linear theory prediction of the maximum F_i for which a steady trapped lee wave is present on the inversion. In (b) the dotted curve bounds the region of parameter space for which lee-wave rotors occur according to linear theory.